Electronic Supplementary Material (ESI) for Dalton Transactions.
This journal is © The Royal Society of Chemistry 2014

A Family of Enantiopure Fe^{III}_4 Single Molecule Magnets: Fine Tuning of Energy Barrier by Remote Substituent

Yuan-Yuan Zhu,[a,b] Chang Cui,[b] Kang Qian,[b] Ji Yin,[a] Bing-Wu Wang,[b]* Zhe-Ming Wang,[b] and Song Gao[b]*

[a]Key Laboratory of Advanced Functional Materials and Devices, Anhui Province, and School of Chemical Engineering, Hefei University of Technology, Hefei, 230009, P. R. China.

[b]Beijing National Laboratory for Molecular Sciences, State Key Laboratory of Rare Earth Materials Chemistry and Applications, College of Chemistry and Molecular Engineering, Peking University, Beijing 100871, P. R. China.

To whom correspondence should be addressed. E-mail: gaosong@pku.edu.cn, wangbw@pku.edu.cn. Fax: (+86) 10-6275-1708.

Synthesis

All starting materials were purchased as reagent grade and were used without further purification.

Synthesis of the Schiff base ligands

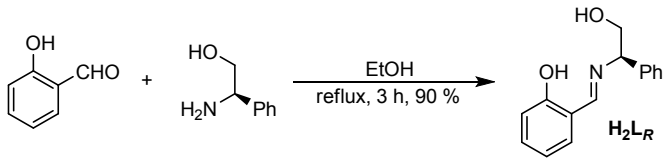

Compound H_2L_R. A solution of salicylaldehyde (1.56 g, 10.0 mmol) and (*R*)-2-amino-2-phenylethanol (1.37 g, 10.0 mmol) in ethanol was stirred under reflux for 2 h and the color of the solution was turned to yellow. After removal of the solvents under reduced pressure, the crude product was purified by recrystallization in the mixture solvent of ethanol and petroleum ether to give compound $\mathbf{L}_R$ as needlelike crystals (2.17 g, 90 %). ^{1}H NMR (400 MHz, $CDCl_3$): δ 13.30 (br, 1 H), 8.48 (s, 1 H), 7.38-7.26 (m, 9 H), 6.98 (d, J = 8.2 Hz, 1 H), 6.89 (t d, J_1 = 7.4 Hz, J_2 = 1.2 Hz, 1 H), 4.47 (t, J = 6.5 Hz, 1 H), 3.92 (d, J = 7.0 Hz, 2 H). Anal. Calcd for $C_{15}H_{15}NO_2$: C, 74.67; H, 6.27; N, 5.81. Found: C, 74.65; H, 6.52; N, 5.73. IR (pure sample): ν = 3225(m), 3088(w), 3031(w), 3008(w), 2970(w), 2952(w), 2930(w), 2920(w), 2863(w), 2734(w), 2664(w), 1949(w), 1924, 1871(w), 1802(w), 1747(w), 1690(w), 1626(s), 1581(m), 1494(m), 1462(m), 1410(m), 1383(m), 1359(w), 1338(w), 1317(w), 1275(s), 1213(w), 1155(m), 1120(w), 1080(m), 1064(m), 1044(m), 1031(m), 1003(w), 979(w), 942(w), 918(w), 905(w), 891(w), 872(w), 853(w), 809(w), 772(m), 764(m), 756(m), 740(w), 694(m), 639(w).

The enantiomer compound $\mathbf{H_2L}_S$ was synthesized by using salicylaldehyde and (*S*)-2-amino-2-phenylethanol as start materials in the same way. ^{1}H NMR (400 MHz, $CDCl_3$): δ 13.32 (br, 1 H), 8.47 (s, 1 H), 7.40-7.25 (m, 9 H), 6.97 (d, J = 8.4 Hz, 1 H), 6.88 (t d, J_1 = 7.4 Hz, J_2 = 1.2 Hz, 1 H), 4.46 (t, J = 6.4 Hz, 1 H), 3.91 (d, J = 7.6 Hz, 2 H). Anal. Calcd for $C_{15}H_{15}NO_2$: C, 74.67; H, 6.27; N, 5.81. Found: C, 74.68; H, 6.51; N, 5.79. IR (pure sample): ν = 3224(m), 3088(w), 3031(w), 3008(w),

2970(w), 2952(w), 2930(w), 2920(w), 2863(w), 2734(w), 2664(w), 1949(w), 1924(w), 1871(w), 1802(w), 1747(w), 1690(w), 1626(s), 1581(m), 1494(m), 1462(m), 1410(m), 1383(m), 1359(w), 1338(w), 1317(w), 1275(s), 1213(w), 1155(m), 1120(w), 1080(m), 1064(m), 1044(m), 1031(m), 1003(w), 979(w), 942(w), 918(w), 905(w), 891(w), 872(w), 853(w), 809(w), 772(m), 764(m), 756(m), 740(w), 694(m), 639(w).

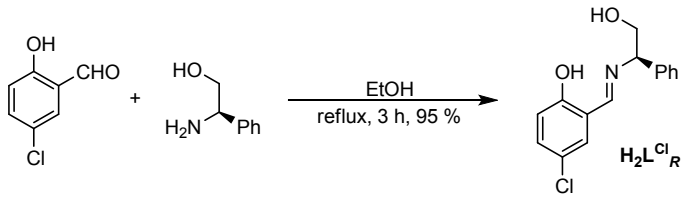

Compound $\mathbf{H_2L^{Cl}_R}$. The compound $\mathbf{H_2L^{Cl}_R}$ was synthesized by using 5-chloro-2-hydroxybenzaldehyde and (*R*)-2-amino-2-phenylethanol as start materials as yellow solid in 95 % yield according to the procedure similar to that for $\mathbf{H_2L_R}$. ^{1}H NMR (400 MHz, $CDCl_3$): δ 13.26 (br, 1 H), 8.41 (s, 1 H), 7.40–7.24 (m, 7 H), 6.92 (d, J = 8.4 Hz, 1 H), 4.49 (t, J = 6.4 Hz, 1 H), 3.93 (d, J = 6.4 Hz, 2 H). Anal. Calcd for $C_{15}H_{14}ClNO_2$: C, 65.34; H, 5.12; N, 5.08. Found: C, 65.16; H, 5.04; N, 5.11. MS (ESI): *m*/*z* 276.10 $[M + 1]^+$. IR (pure sample): ν = 3472(m), 3425(m), 3107(w), 3088(w), 3060(w), 3029(w), 2973(w), 2952(w), 2917(w), 2891(w), 2866(w), 2748(w), 2681(w), 2631(w), 1958(w), 1887(w), 1819(w), 1769(w), 1704(w), 1635(s), 1573(m), 1513(m), 1481(s), 1453(m), 1377(s), 1341(w), 1308(w), 1281(s), 1222(m), 1209(m), 1182(m), 1122(w), 1095(m), 1059(s), 1030(m), 989(w), 973(w), 918(m), 925(m), 893(m), 856(s), 831(s), 804(m), 780(m), 767(s), 734(w), 705(s), 644(m).

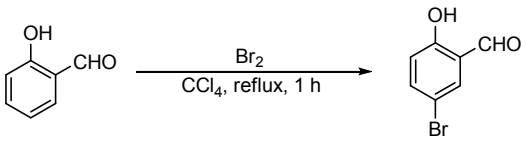

Compound 5-bromo-2-hydroxybenzaldehyde was synthesizd according to the literature method.[1] ^{1}H NMR (400 MHz, $CDCl_3$): δ 10.93 (s, 1 H), 9.84 (s, H), 7.68 (d, J = 2.4 Hz, 1 H), 7.60 (d d, J_1 =

8.8 Hz, J_2 = 2.4 Hz, 1 H), 6.91 (d, J = 8.8 Hz).

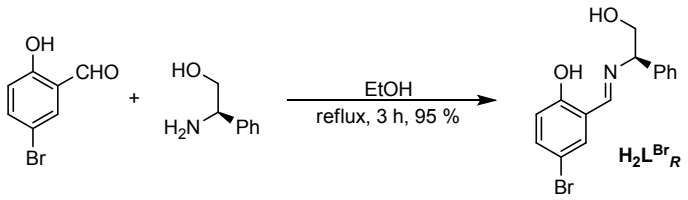

Compound $\mathbf{H_2L^{Br}_R}$. The compound $\mathbf{H_2L^{Br}_R}$ was synthesized by using 5-bromo-2-hydroxybenzaldehyde and (*R*)-2-amino-2-phenylethanol as start materials as yellow solid in 95 % yield according to the procedure similar to that for $\mathbf{H_2L_R}$. ^{1}H NMR (400 MHz, $CDCl_3$): δ 13.30 (br, 1 H), 8.40 (s, 1 H), 7.41–7.29 (m, 7 H), 6.87 (d, J = 8.4 Hz, 1 H), 4.48 (t, J = 6.4 Hz, 1 H), 3.93 (d, J = 6.4 Hz, 2 H). Anal. Calcd for $C_{15}H_{14}BrNO_2$: C, 56.27; H, 4.41; N, 4.37. Found: C, 56.13; H, 4.35; N, 4.35. MS (ESI): m/z 320.08 $[M + 1]^+$. IR (pure sample): v = 3480(m), 3417(m), 3085(w), 3060(w), 3028(w), 3004(w), 2983(w), 2969(w), 2923(w), 2882(w), 2865(w), 2743(w), 2682(w), 1952(w), 1881(w), 1831(w), 1812(w), 1770(w), 1698(w), 1630(s), 1570(m), 1476(s), 1454(m), 1374(m), 1340(w), 1313(w), 1280(s), 1222(w), 1207(m), 1184(m), 1130(w), 1078(m), 1057(m), 1033(m), 1028(m), 1000(w), 985(w), 974(w), 948(w), 915(m), 894(m), 854(w), 825(s), 810(m), 778(w), 764(m), 734(w), 699(m), 681(w), 640(w), 626(w).

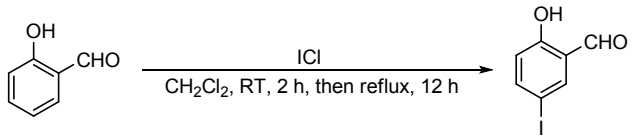

Compound 2-hydroxy-5-iodobenzaldehyde was synthesizd according to the literature method.[2] ^{1}H NMR (400 MHz, $CDCl_3$): δ 10.94 (s, 1 H), 9.83 (s, 1 H), 7.85 (*d*, J = 2.0 Hz, 1 H), 7.77 (*d*, J = 8.4 Hz, 1 H), 6.80 (*d*, J = 8.4 Hz, 1 H).

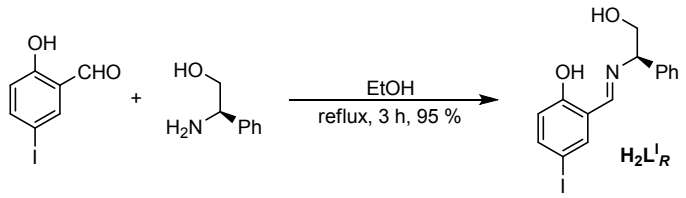

Compound $H_2L^I_R$. The compound $\mathbf{H_2L^I_R}$ was synthesized by using 2-hydroxy-5-iodobenzaldehyde and (*R*)-2-amino-2-phenylethanol as start materials as yellow solid in 95 % yield according to the procedure similar to that for $\mathbf{H_2L_R}$. ^{1}H NMR (400 MHz, $CDCl_3$): δ 13.34 (br, 1 H), 8.38 (s, 1 H), 7.56 (d, J = 9.6 Hz, 1 H), 7.55 (s, 1 H), 7.40—7.31 (m, 5 H), 4.48 (t, J = 6.4 Hz, 1 H), 3.93 (d, J = 6.4 Hz, 2 H). Anal. Calcd for $C_{15}H_{14}INO_2$: C, 49.07; H, 3.84; N, 3.81. Found: C, 49.57; H, 3.96; N, 3.81. MS (ESI): *m*/*z* 368.10 $[M + 1]^+$. IR (pure sample): v = 3481(m), 3419(m), 3101(w), 3084(w), 3059(w), 3026(w), 3003(w), 2968(w), 2923(w), 2883(w), 2865(w), 2741(w), 2607(w), 1968(w), 1951(w), 1886(w), 1831(w), 1811(w), 1770(w), 1628(s), 1601(m), 1566(m), 1492(m), 1474(m), 1453(m), 1371(s), 1340(w), 1313(w), 1280(s), 1222(w), 1205(m), 1183(m), 1161(w), 1132(w), 1088(m), 1075(m), 1058(s), 1033(m), 1029(m), 1000(w), 914(m), 895(w), 852(w), 823(s), 777(w), 763(m), 734(w), 699(m), 671(w), 639(w), 615(w).

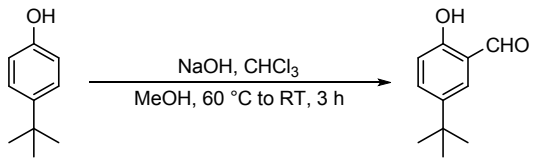

Compound 5-*tert*-butyl-2-hydroxybenzaldehyde was synthesizd according to the literature method.[3] ^{1}H NMR (400 MHz, $CDCl_3$): δ 10.86 (s, 1 H), 9.89 (s, 1 H), 7.58 (d d, J_1 = 8.8 Hz, J_2 = 2.0 Hz, 1 H), 7.51 (d, J = 2.4 Hz, 1 H), 1.33 (s, 9 H).

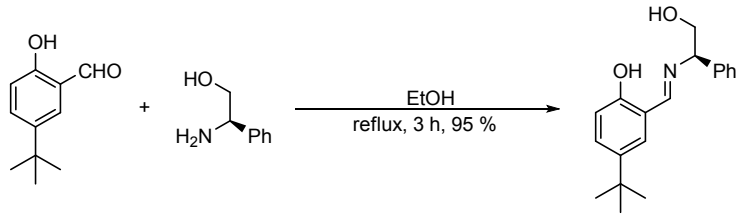

Compound $H_2L^{t\text{-}Bu}_R$. The compound $\mathbf{H_2L^{t\text{-}Bu}_R}$ was synthesized by using 5-*tert*-butyl-2-

hydroxybenzaldehyde and (*R*)-2-amino-2-phenylethanol as start materials as yellow solid in 95 % yield according to the procedure similar to that for $\mathbf{H_2L_R}$. ^{1}H NMR (400 MHz, $CDCl_3$): δ 13.01 (br, 1 H), 8.50 (s, 1 H), 7.39–7.26 (m, 7 H), 6.93 (d, J = 8.4 Hz, 1 H), 4.48 (t, J = 6.4 Hz, 1 H), 3.93 (d, J = 6.4 Hz, 2 H). MS (ESI): m/z 298.22 $[M + 1]^+$. Anal. Calcd for $C_{15}H_{14}BrNO_2$: C, 76.73; H, 7.80; N, 4.71. Found: C, 76.59; H, 7.77; N, 4.67. IR (pure sample): ν = 3250(m), 3087(w), 3063(w), 3032(w), 2965(m), 2929(w), 2878(w), 2823(w), 2645(w), 1959(w), 1942(w), 1915(w), 1884(w), 1868(w), 1799(w), 1764(w), 1743(w), 1722(w), 1627(s), 1590(m), 1500(m), 1492(m), 1464(m), 1454(m), 1396(m), 1383(m), 1362(w), 1336(w), 1314(w), 1288(m), 1266(m), 1247(w), 1210(w), 1189(w), 1153(w), 1139(w), 1106(w), 1077(m), 1063(m), 1036(m), 1027(m), 982(w), 959(w), 936(w), 907(m), 885(w), 858(w), 829(m), 821(m), 785(w), 763(m), 744(w), 694(m), 656(w), 640(w), 614(w).

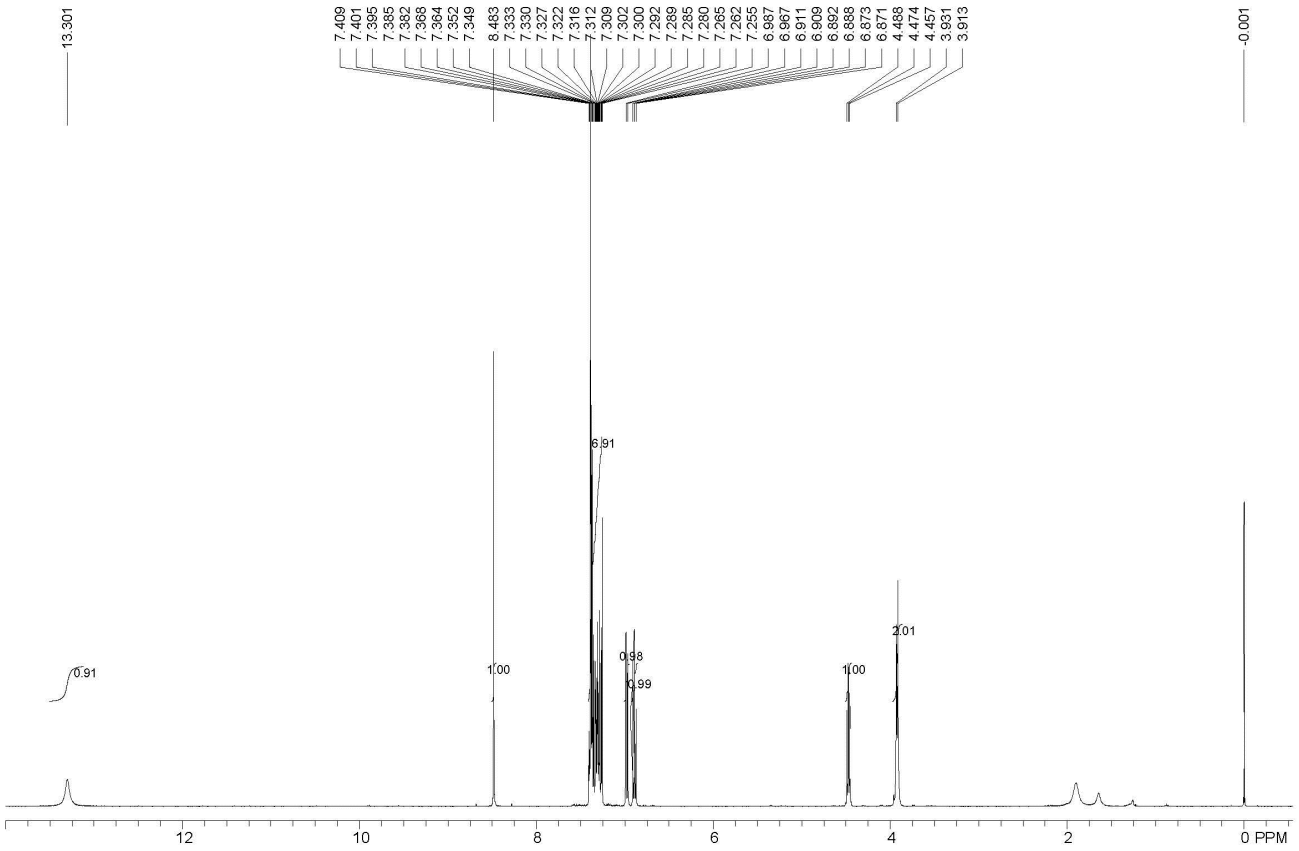

Figure S1. ^{1}H NMR spectrum of $\mathbf{H_2L_R}$ (400 MHz) in $CDCl_3$ (10 mM).

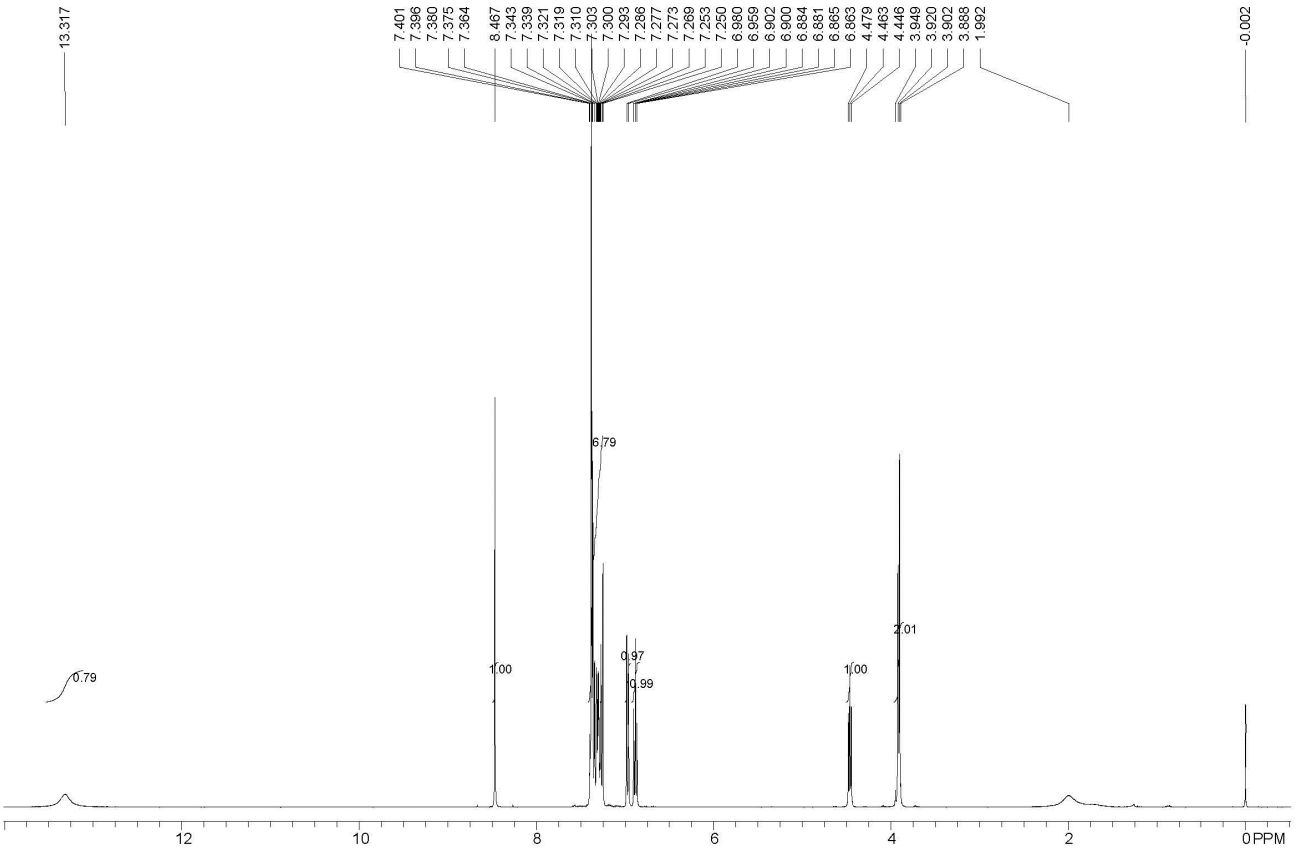

Figure S2. ^{1}H NMR spectrum of $\mathbf{H_2L}_{\boldsymbol{S}}$ (400 MHz) in $CDCl_3$ (10 mM).

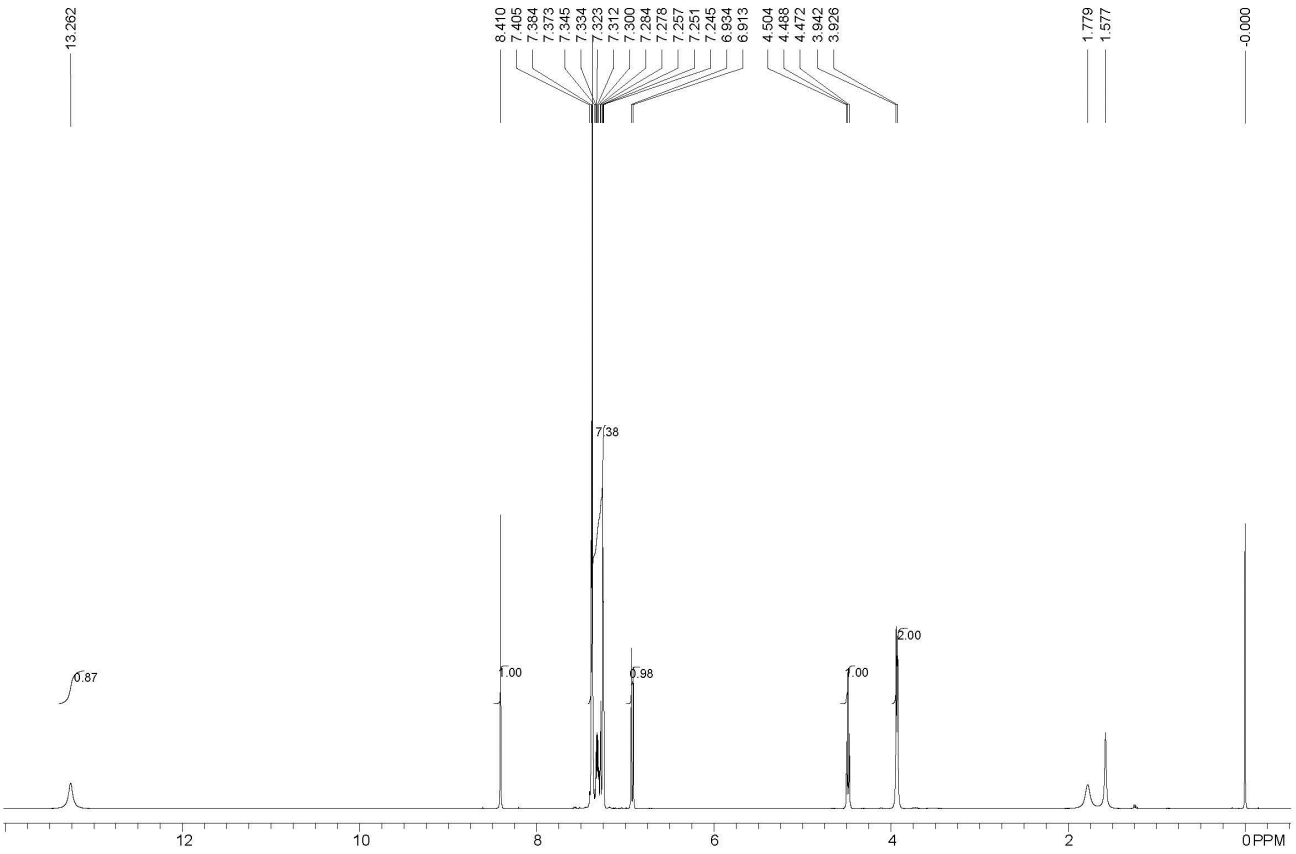

Figure S3. ^{1}H NMR spectrum of $\mathbf{H_2L^{Cl}}_{\boldsymbol{R}}$ (400 MHz) in $CDCl_3$ (10 mM).

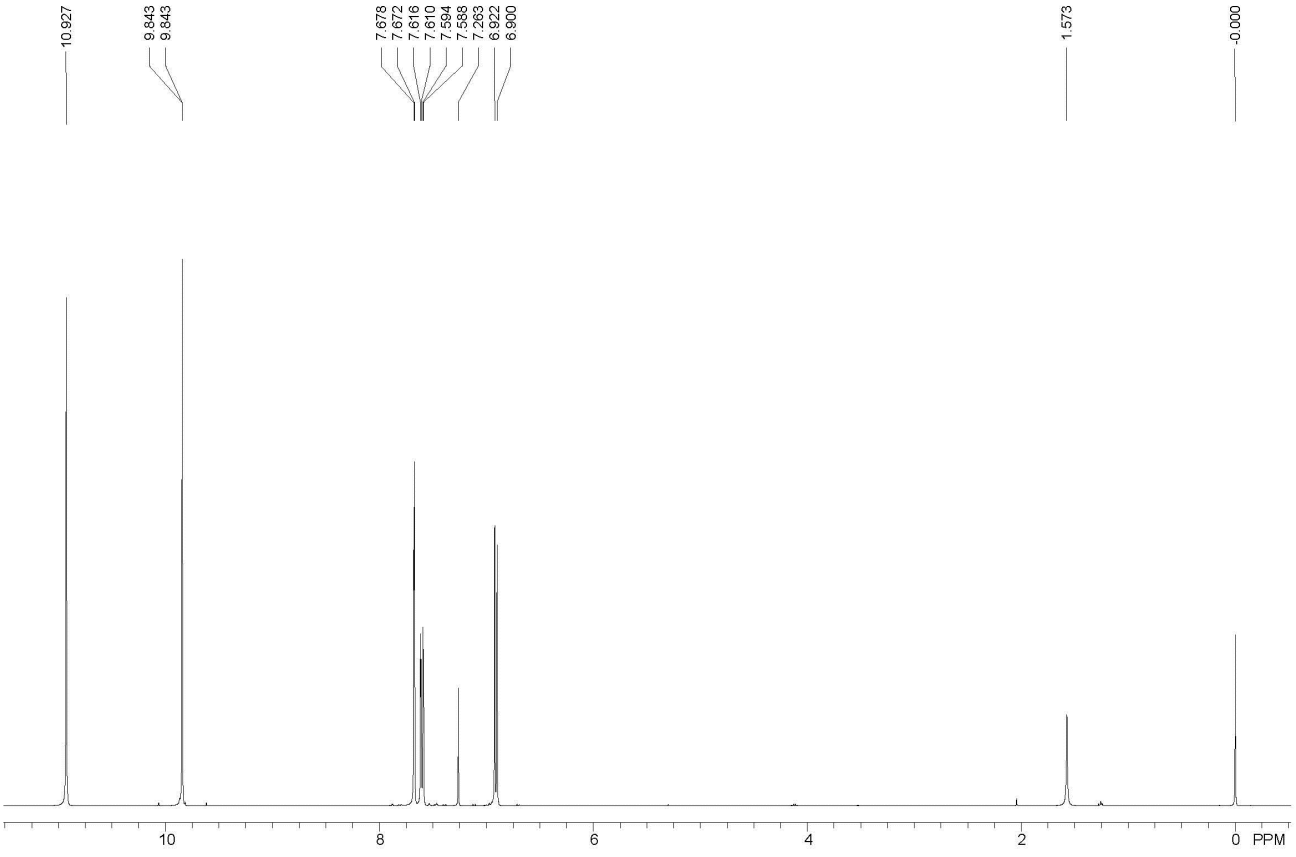

Figure S4. ^{1}H NMR spectrum of **5-bromo-2-hydroxybenzaldehyde** (400 MHz) in $CDCl_3$ (10 mM).

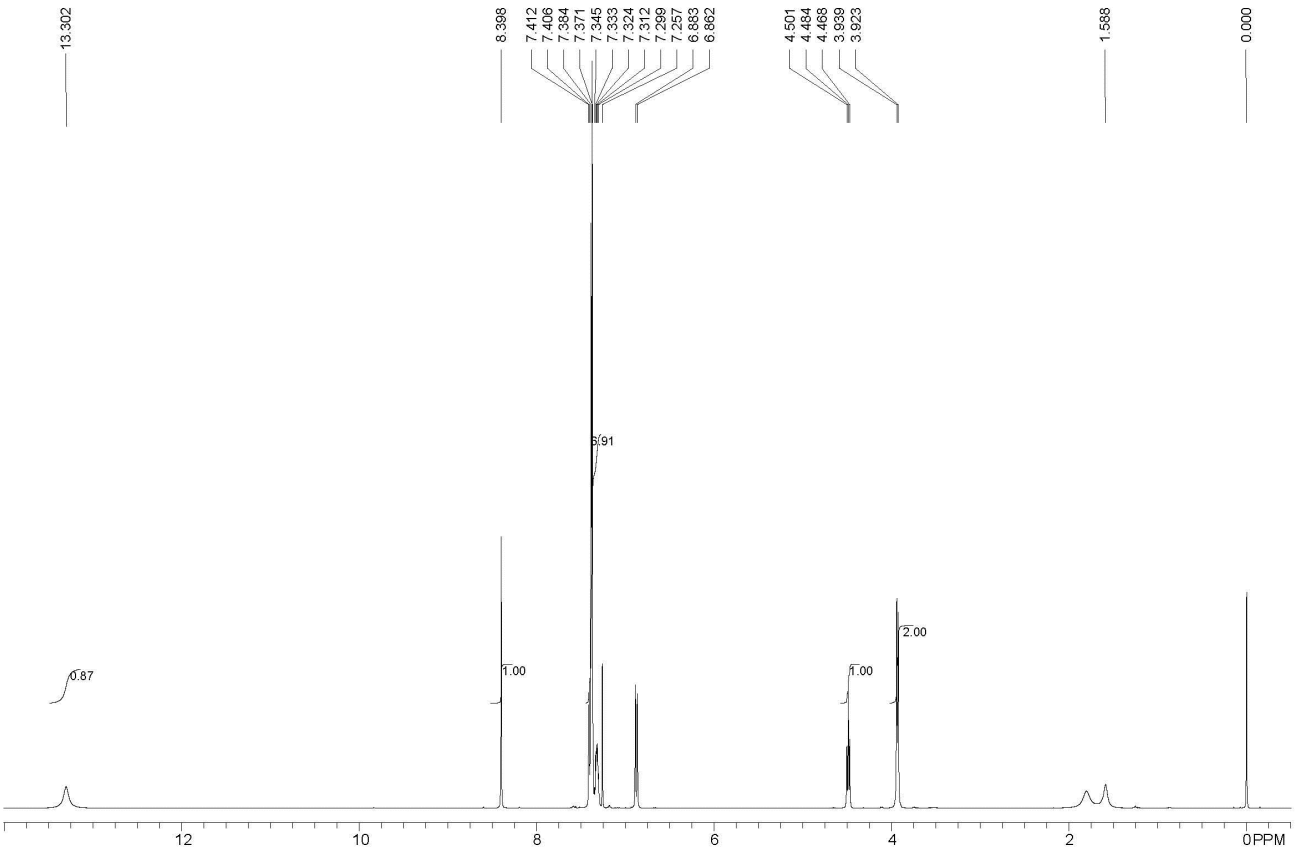

Figure S5. ^{1}H NMR spectrum of $\mathbf{H_2L^{Br}}_{\boldsymbol{R}}$ (400 MHz) in $CDCl_3$ (10 mM).

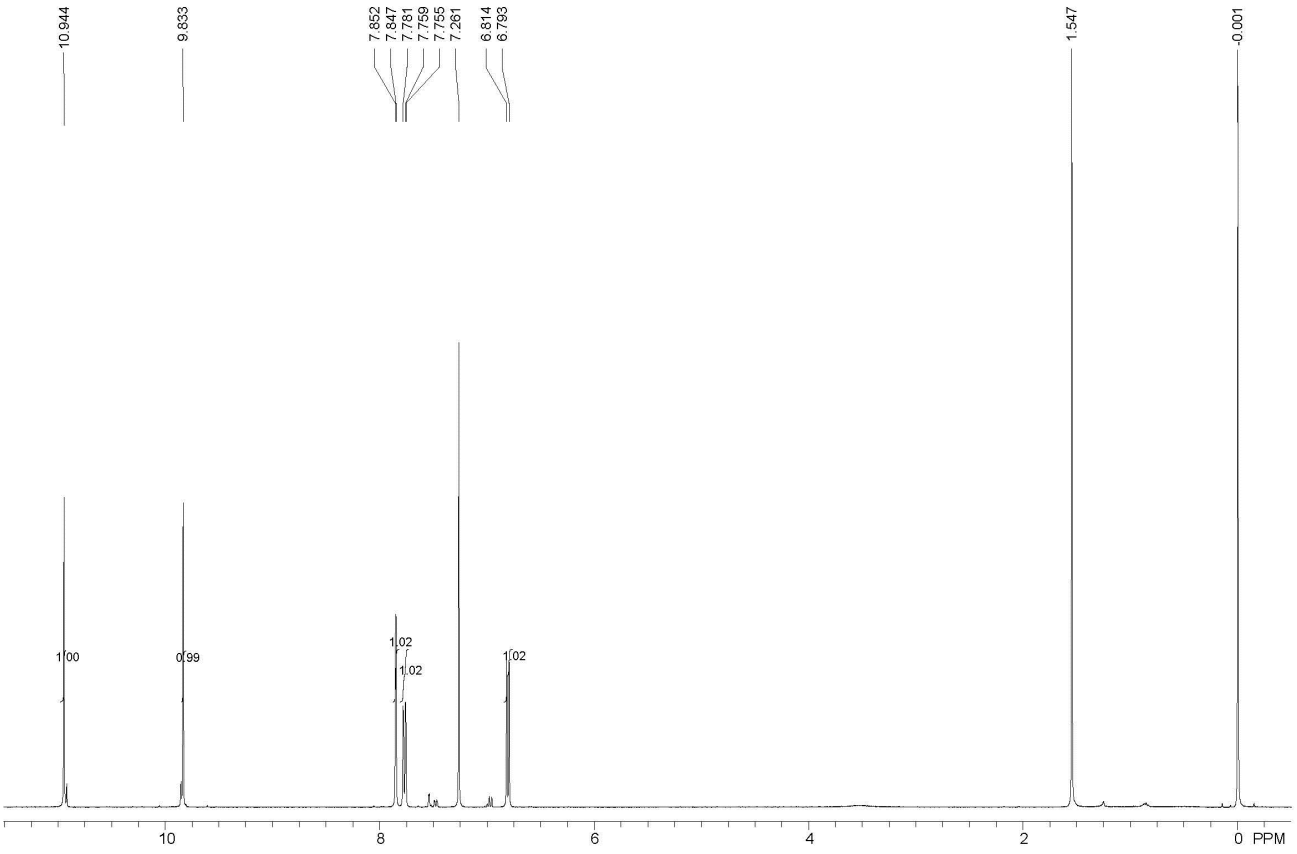

Figure S6. ^{1}H NMR spectrum of **2-hydroxy-5-iodobenzaldehyde** (400 MHz) in $CDCl_3$ (10 mM).

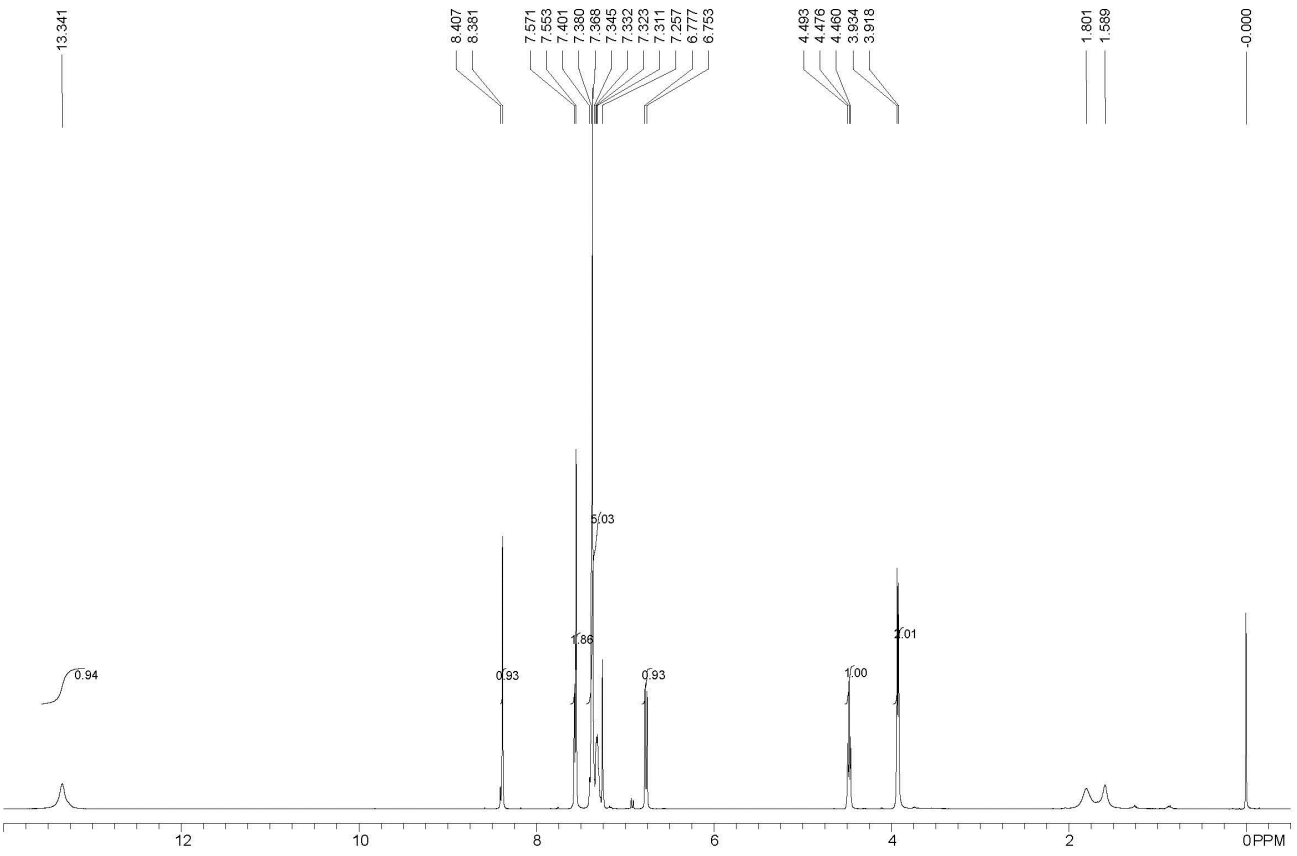

Figure S7. ^{1}H NMR spectrum of $\mathbf{H_2L^I}_{\boldsymbol{R}}$ (400 MHz) in $CDCl_3$ (10 mM).

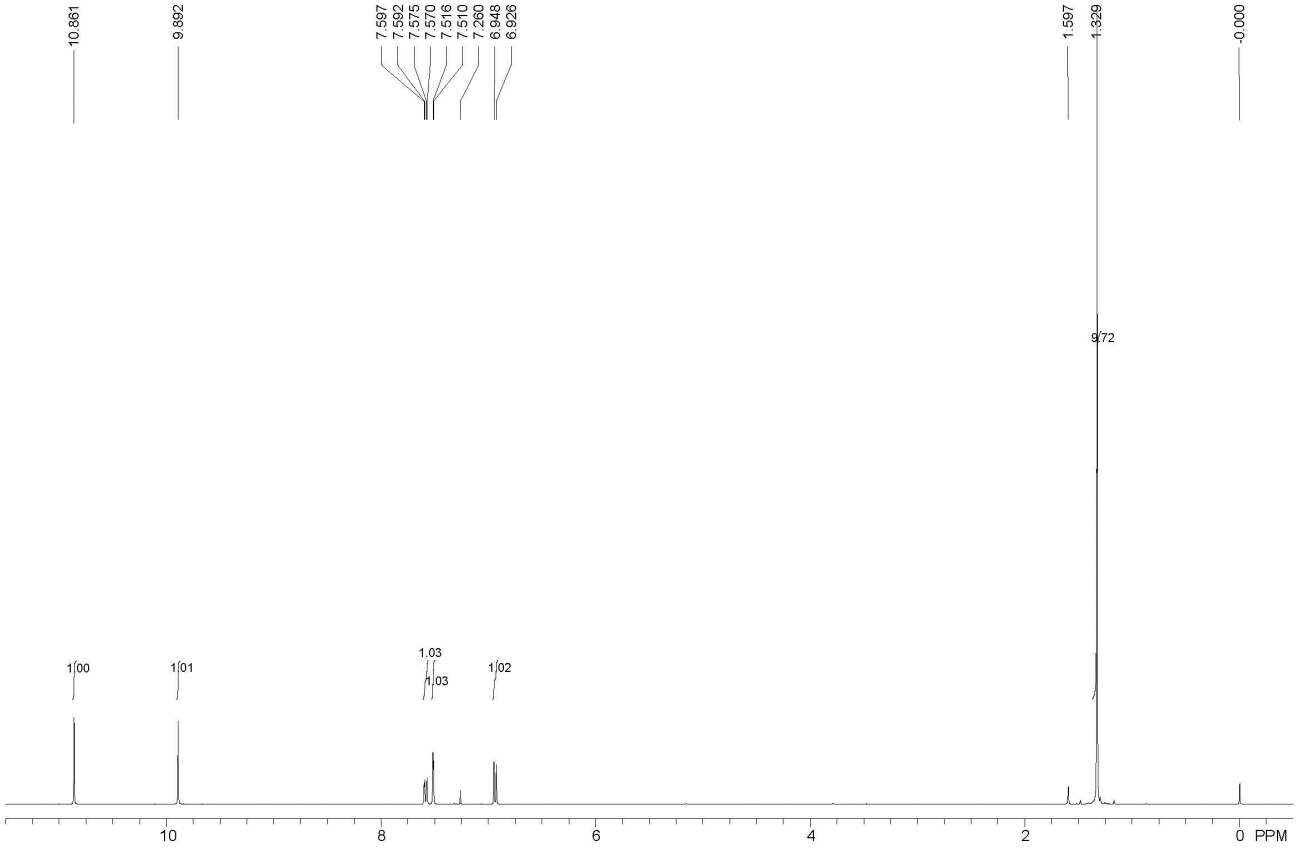

Figure S8. ^{1}H NMR spectrum of **5-*tert*-butyl-2-hydroxybenzaldehyde** (400 MHz) in $CDCl_3$ (10 mM).

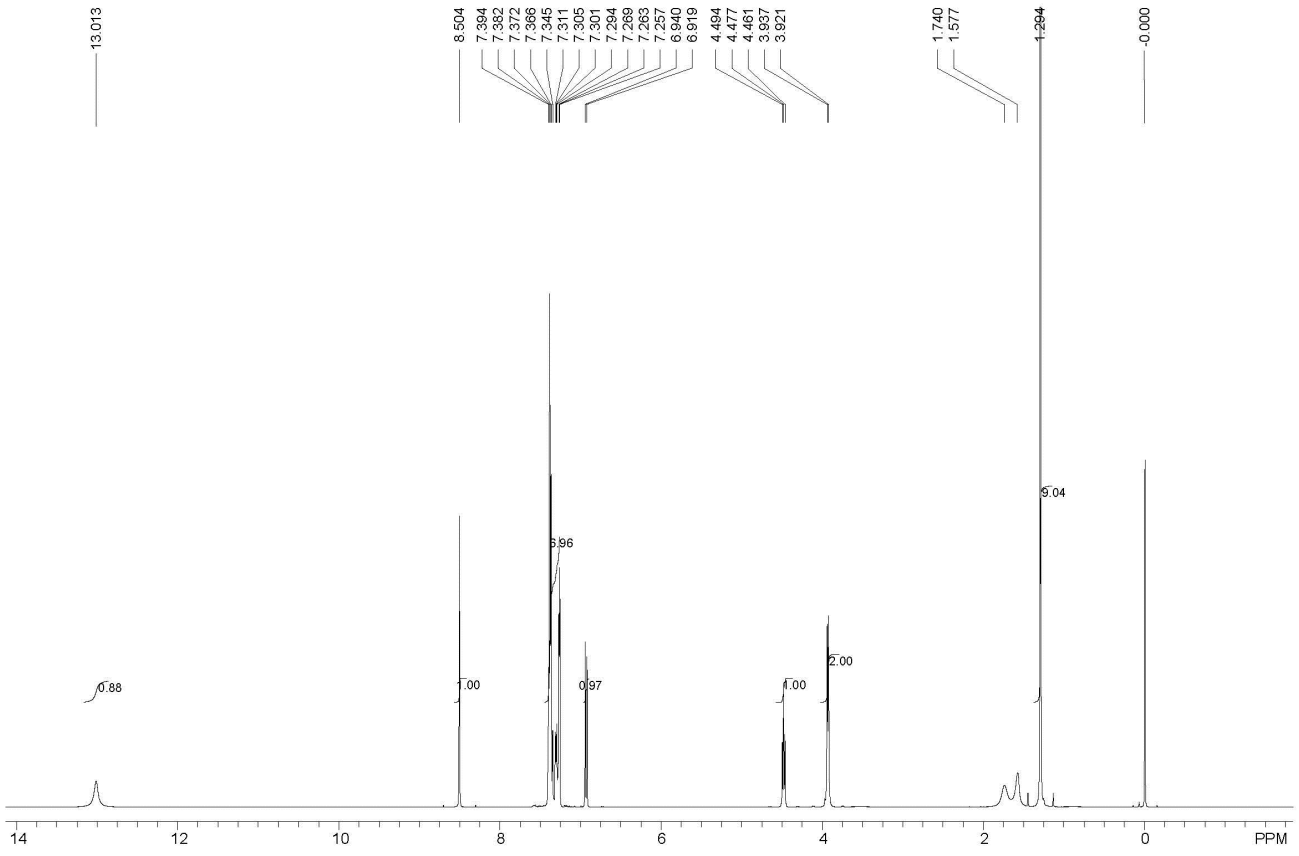

Figure S9. ^{1}H NMR spectrum of $\mathbf{H_2L^{tBu}_{\boldsymbol{R}}}$ (400 MHz) in $CDCl_3$ (10 mM).

Table S1. Selected bond lengths (Å) and angles (°) for **2*R***.

Fe(1)-O(10)	2.005(4)	Fe(3)-O(7)	1.916(4)
Fe(1)-O(8)	2.018(4)	Fe(3)-O(5)	1.936(4)
Fe(1)-O(2)	2.030(4)	Fe(3)-O(8)	2.005(4)
Fe(1)-O(4)	2.034(4)	Fe(3)-O(6)	2.011(4)
Fe(1)-O(6)	2.045(4)	Fe(3)-N(4)	2.134(4)
Fe(1)-O(12)	2.048(4)	Fe(3)-N(3)	2.151(5)
Fe(2)-O(3)	1.919(4)	Fe(4)-O(9)	1.939(4)
Fe(2)-O(1)	1.936(4)	Fe(4)-O(11)	1.942(4)
Fe(2)-O(2)	2.010(4)	Fe(4)-O(10)	2.000(4)
Fe(2)-O(4)	2.018(4)	Fe(4)-O(12)	2.025(4)
Fe(2)-N(1)	2.132(4)	Fe(4)-N(6)	2.139(4)
Fe(2)-N(2)	2.147(4)	Fe(4)-N(5)	2.141(4)
O(10)-Fe(1)-O(8)	127.47(15)	O(7)-Fe(3)-O(5)	101.71(18)
O(10)-Fe(1)-O(2)	88.61(15)	O(7)-Fe(3)-O(8)	156.68(16)
O(8)-Fe(1)-O(2)	137.11(15)	O(5)-Fe(3)-O(8)	94.79(17)
O(10)-Fe(1)-O(4)	137.76(15)	O(7)-Fe(3)-O(6)	95.56(17)
O(8)-Fe(1)-O(4)	88.29(14)	O(5)-Fe(3)-O(6)	156.34(16)
O(2)-Fe(1)-O(4)	73.42(14)	O(8)-Fe(3)-O(6)	74.14(14)
O(10)-Fe(1)-O(6)	89.59(15)	O(7)-Fe(3)-N(4)	86.45(17)
O(8)-Fe(1)-O(6)	73.12(14)	O(5)-Fe(3)-N(4)	90.77(17)
O(2)-Fe(1)-O(6)	86.58(14)	O(8)-Fe(3)-N(4)	76.88(16)
O(4)-Fe(1)-O(6)	125.88(15)	O(6)-Fe(3)-N(4)	106.45(16)
O(10)-Fe(1)-O(12)	72.91(15)	O(7)-Fe(3)-N(3)	92.79(17)
O(8)-Fe(1)-O(12)	87.17(14)	O(5)-Fe(3)-N(3)	86.14(17)
O(2)-Fe(1)-O(12)	129.86(15)	O(8)-Fe(3)-N(3)	104.77(16)
O(4)-Fe(1)-O(12)	89.58(15)	O(6)-Fe(3)-N(3)	76.92(16)
O(6)-Fe(1)-O(12)	137.53(15)	N(4)-Fe(3)-N(3)	176.60(17)
O(3)-Fe(2)-O(1)	100.95(18)	O(9)-Fe(4)-O(11)	101.36(18)
O(3)-Fe(2)-O(2)	92.43(16)	O(9)-Fe(4)-O(10)	154.59(16)
O(1)-Fe(2)-O(2)	160.08(17)	O(11)-Fe(4)-O(10)	96.74(16)
O(3)-Fe(2)-O(4)	153.47(17)	O(9)-Fe(4)-O(12)	94.68(16)
O(1)-Fe(2)-O(4)	98.54(16)	O(11)-Fe(4)-O(12)	158.04(16)
O(2)-Fe(2)-O(4)	74.18(14)	O(10)-Fe(4)-O(12)	73.49(15)
O(3)-Fe(2)-N(1)	96.37(17)	O(9)-Fe(4)-N(6)	96.96(17)
O(1)-Fe(2)-N(1)	86.09(16)	O(11)-Fe(4)-N(6)	85.40(16)
O(2)-Fe(2)-N(1)	77.74(15)	O(10)-Fe(4)-N(6)	102.16(16)
O(4)-Fe(2)-N(1)	102.78(16)	O(12)-Fe(4)-N(6)	77.78(15)
O(3)-Fe(2)-N(2)	86.40(17)	O(9)-Fe(4)-N(5)	86.03(17)
O(1)-Fe(2)-N(2)	85.90(16)	O(11)-Fe(4)-N(5)	89.19(17)
O(2)-Fe(2)-N(2)	109.83(15)	O(10)-Fe(4)-N(5)	76.49(16)
O(4)-Fe(2)-N(2)	77.20(16)	O(12)-Fe(4)-N(5)	106.95(16)
N(1)-Fe(2)-N(2)	171.88(17)	N(6)-Fe(4)-N(5)	174.24(17)

Table S2. Selected bond lengths (Å) and angles (°) for **2*S***.

Fe(1)-O(10)	2.004(4)	Fe(3)-O(7)	1.917(5)
Fe(1)-O(8)	2.021(4)	Fe(3)-O(5)	1.949(4)
Fe(1)-O(2)	2.034(4)	Fe(3)-O(6)	2.010(4)
Fe(1)-O(4)	2.040(4)	Fe(3)-O(8)	2.014(5)
Fe(1)-O(12)	2.045(4)	Fe(3)-N(4)	2.148(6)
Fe(1)-O(6)	2.047(4)	Fe(3)-N(3)	2.155(6)
Fe(2)-O(3)	1.934(5)	Fe(4)-O(9)	1.941(5)
Fe(2)-O(1)	1.941(5)	Fe(4)-O(11)	1.944(5)
Fe(2)-O(2)	2.008(4)	Fe(4)-O(10)	2.003(5)
Fe(2)-O(4)	2.018(4)	Fe(4)-O(12)	2.032(4)
Fe(2)-N(1)	2.128(5)	Fe(4)-N(6)	2.134(5)
Fe(2)-N(2)	2.160(5)	Fe(4)-N(5)	2.142(5)
O(10)-Fe(1)-O(8)	127.68(18)	O(7)-Fe(3)-O(5)	101.4(2)
O(10)-Fe(1)-O(2)	88.70(17)	O(7)-Fe(3)-O(6)	95.8(2)
O(8)-Fe(1)-O(2)	136.92(18)	O(5)-Fe(3)-O(6)	156.30(19)
O(10)-Fe(1)-O(4)	137.71(19)	O(7)-Fe(3)-O(8)	157.2(2)
O(8)-Fe(1)-O(4)	88.09(18)	O(5)-Fe(3)-O(8)	94.8(2)
O(2)-Fe(1)-O(4)	73.39(17)	O(6)-Fe(3)-O(8)	74.11(17)
O(10)-Fe(1)-O(12)	73.07(18)	O(7)-Fe(3)-N(4)	86.9(2)
O(8)-Fe(1)-O(12)	87.22(17)	O(5)-Fe(3)-N(4)	91.0(2)
O(2)-Fe(1)-O(12)	129.77(18)	O(6)-Fe(3)-N(4)	106.19(19)
O(4)-Fe(1)-O(12)	89.27(18)	O(8)-Fe(3)-N(4)	76.82(19)
O(10)-Fe(1)-O(6)	89.53(18)	O(7)-Fe(3)-N(3)	92.5(2)
O(8)-Fe(1)-O(6)	73.16(17)	O(5)-Fe(3)-N(3)	85.7(2)
O(2)-Fe(1)-O(6)	86.75(18)	O(6)-Fe(3)-N(3)	77.29(19)
O(4)-Fe(1)-O(6)	126.08(19)	O(8)-Fe(3)-N(3)	104.76(19)
O(12)-Fe(1)-O(6)	137.58(18)	N(4)-Fe(3)-N(3)	176.5(2)
O(3)-Fe(2)-O(1)	101.0(2)	O(9)-Fe(4)-O(11)	101.2(2)
O(3)-Fe(2)-O(2)	92.2(2)	O(9)-Fe(4)-O(10)	154.53(19)
O(1)-Fe(2)-O(2)	160.3(2)	O(11)-Fe(4)-O(10)	96.8(2)
O(3)-Fe(2)-O(4)	153.5(2)	O(9)-Fe(4)-O(12)	94.88(19)
O(1)-Fe(2)-O(4)	98.4(2)	O(11)-Fe(4)-O(12)	158.13(19)
O(2)-Fe(2)-O(4)	74.41(17)	O(10)-Fe(4)-O(12)	73.37(17)
O(3)-Fe(2)-N(1)	96.2(2)	O(9)-Fe(4)-N(6)	97.0(2)
O(1)-Fe(2)-N(1)	86.4(2)	O(11)-Fe(4)-N(6)	85.5(2)
O(2)-Fe(2)-N(1)	77.62(18)	O(10)-Fe(4)-N(6)	102.3(2)
O(4)-Fe(2)-N(1)	102.8(2)	O(12)-Fe(4)-N(6)	77.87(18)
O(3)-Fe(2)-N(2)	86.3(2)	O(9)-Fe(4)-N(5)	85.8(2)
O(1)-Fe(2)-N(2)	85.9(2)	O(11)-Fe(4)-N(5)	89.0(2)
O(2)-Fe(2)-N(2)	109.75(19)	O(10)-Fe(4)-N(5)	76.6(2)
O(4)-Fe(2)-N(2)	77.3(2)	O(12)-Fe(4)-N(5)	106.96(19)
N(1)-Fe(2)-N(2)	172.2(2)	N(6)-Fe(4)-N(5)	174.2(2)

Table S3. Selected bond lengths (Å) and angles (°) for **3*R***.

Fe(1)-O(2)	2.007(6)	Fe(3)-O(12)	1.934(6)
Fe(1)-O(3)	2.011(6)	Fe(3)-O(11)	1.957(6)
Fe(1)-O(6)	2.021(6)	Fe(3)-O(3)	2.008(6)
Fe(1)-O(5)	2.028(6)	Fe(3)-O(4)	2.008(6)
Fe(1)-O(1)	2.030(6)	Fe(3)-N(4)	2.140(8)
Fe(1)-O(4)	2.049(6)	Fe(3)-N(3)	2.157(8)
Fe(2)-O(8)	1.930(6)	Fe(4)-O(10)	1.931(6)
Fe(2)-O(7)	1.933(6)	Fe(4)-O(9)	1.939(7)
Fe(2)-O(2)	1.995(6)	Fe(4)-O(5)	1.997(6)
Fe(2)-O(1)	2.010(6)	Fe(4)-O(6)	2.039(6)
Fe(2)-N(1)	2.146(7)	Fe(4)-N(5)	2.146(8)
Fe(2)-N(2)	2.175(7)	Fe(4)-N(6)	2.161(8)
O(2)-Fe(1)-O(3)	88.7(3)	O(12)-Fe(3)-O(11)	104.5(3)
O(2)-Fe(1)-O(6)	138.0(3)	O(12)-Fe(3)-O(3)	155.4(3)
O(3)-Fe(1)-O(6)	125.6(3)	O(11)-Fe(3)-O(3)	93.5(3)
O(2)-Fe(1)-O(5)	86.8(2)	O(12)-Fe(3)-O(4)	94.5(3)
O(3)-Fe(1)-O(5)	87.0(3)	O(11)-Fe(3)-O(4)	154.2(3)
O(6)-Fe(1)-O(5)	73.4(2)	O(3)-Fe(3)-O(4)	74.3(2)
O(2)-Fe(1)-O(1)	73.2(2)	O(12)-Fe(3)-N(4)	86.0(3)
O(3)-Fe(1)-O(1)	139.3(2)	O(11)-Fe(3)-N(4)	89.9(3)
O(6)-Fe(1)-O(1)	89.3(2)	O(3)-Fe(3)-N(4)	77.4(3)
O(5)-Fe(1)-O(1)	126.7(2)	O(4)-Fe(3)-N(4)	108.9(3)
O(2)-Fe(1)-O(4)	125.6(2)	O(12)-Fe(3)-N(3)	90.7(3)
O(3)-Fe(1)-O(4)	73.4(2)	O(11)-Fe(3)-N(3)	85.3(3)
O(6)-Fe(1)-O(4)	90.4(2)	O(3)-Fe(3)-N(3)	107.6(3)
O(5)-Fe(1)-O(4)	140.4(2)	O(4)-Fe(3)-N(3)	77.1(2)
O(1)-Fe(1)-O(4)	87.8(2)	N(4)-Fe(3)-N(3)	173.3(3)
O(8)-Fe(2)-O(7)	102.7(3)	O(10)-Fe(4)-O(9)	101.8(3)
O(8)-Fe(2)-O(2)	95.1(3)	O(10)-Fe(4)-O(5)	94.2(3)
O(7)-Fe(2)-O(2)	155.1(3)	O(9)-Fe(4)-O(5)	155.7(3)
O(8)-Fe(2)-O(1)	155.9(3)	O(10)-Fe(4)-O(6)	155.8(3)
O(7)-Fe(2)-O(1)	95.1(3)	O(9)-Fe(4)-O(6)	96.9(3)
O(2)-Fe(2)-O(1)	73.9(2)	O(5)-Fe(4)-O(6)	73.7(2)
O(8)-Fe(2)-N(1)	86.1(3)	O(10)-Fe(4)-N(5)	86.9(3)
O(7)-Fe(2)-N(1)	92.5(3)	O(9)-Fe(4)-N(5)	93.0(3)
O(2)-Fe(2)-N(1)	106.1(3)	O(5)-Fe(4)-N(5)	106.0(3)
O(1)-Fe(2)-N(1)	76.8(2)	O(6)-Fe(4)-N(5)	76.8(3)
O(8)-Fe(2)-N(2)	90.4(3)	O(10)-Fe(4)-N(6)	91.2(3)
O(7)-Fe(2)-N(2)	85.9(3)	O(9)-Fe(4)-N(6)	85.4(3)
O(2)-Fe(2)-N(2)	76.6(3)	O(5)-Fe(4)-N(6)	76.0(3)
O(1)-Fe(2)-N(2)	107.2(2)	O(6)-Fe(4)-N(6)	105.5(3)
N(1)-Fe(2)-N(2)	175.8(3)	N(5)-Fe(4)-N(6)	177.3(3)

Table S4. Selected bond lengths (Å) and angles (°) for **4*R***.

Fe(1)-O(4)	2.008(5)	Fe(3)-O(5)	1.933(6)
Fe(1)-O(6)	2.016(5)	Fe(3)-O(7)	1.934(6)
Fe(1)-O(12)	2.020(6)	Fe(3)-O(8)	1.998(6)
Fe(1)-O(8)	2.023(6)	Fe(3)-O(6)	2.035(5)
Fe(1)-O(10)	2.037(5)	Fe(3)-N(3)	2.144(7)
Fe(1)-O(2)	2.046(5)	Fe(3)-N(4)	2.153(7)
Fe(2)-O(1)	1.931(6)	Fe(4)-O(9)	1.944(6)
Fe(2)-O(3)	1.935(6)	Fe(4)-O(11)	1.946(6)
Fe(2)-O(4)	1.984(6)	Fe(4)-O(12)	1.998(5)
Fe(2)-O(2)	2.012(5)	Fe(4)-O(10)	2.006(6)
Fe(2)-N(2)	2.137(7)	Fe(4)-N(5)	2.140(6)
Fe(2)-N(1)	2.158(7)	Fe(4)-N(6)	2.173(6)
O(4)-Fe(1)-O(6)	125.6(2)	O(5)-Fe(3)-O(7)	101.9(3)
O(4)-Fe(1)-O(12)	88.4(2)	O(5)-Fe(3)-O(8)	94.9(2)
O(6)-Fe(1)-O(12)	138.8(2)	O(7)-Fe(3)-O(8)	155.8(3)
O(4)-Fe(1)-O(8)	88.2(2)	O(5)-Fe(3)-O(6)	156.0(3)
O(6)-Fe(1)-O(8)	73.6(2)	O(7)-Fe(3)-O(6)	96.0(3)
O(12)-Fe(1)-O(8)	86.4(2)	O(8)-Fe(3)-O(6)	73.7(2)
O(4)-Fe(1)-O(10)	138.1(2)	O(5)-Fe(3)-N(3)	86.3(3)
O(6)-Fe(1)-O(10)	89.8(2)	O(7)-Fe(3)-N(3)	91.8(3)
O(12)-Fe(1)-O(10)	73.5(2)	O(8)-Fe(3)-N(3)	106.7(2)
O(8)-Fe(1)-O(10)	126.6(2)	O(6)-Fe(3)-N(3)	77.2(2)
O(4)-Fe(1)-O(2)	73.1(2)	O(5)-Fe(3)-N(4)	92.3(3)
O(6)-Fe(1)-O(2)	89.9(2)	O(7)-Fe(3)-N(4)	86.4(3)
O(12)-Fe(1)-O(2)	125.5(2)	O(8)-Fe(3)-N(4)	75.5(2)
O(8)-Fe(1)-O(2)	141.2(2)	O(6)-Fe(3)-N(4)	104.7(2)
O(10)-Fe(1)-O(2)	87.0(2)	N(3)-Fe(3)-N(4)	177.5(3)
O(1)-Fe(2)-O(3)	105.1(3)	O(9)-Fe(4)-O(11)	102.7(3)
O(1)-Fe(2)-O(4)	93.7(3)	O(9)-Fe(4)-O(12)	94.7(2)
O(3)-Fe(2)-O(4)	154.5(3)	O(11)-Fe(4)-O(12)	155.3(2)
O(1)-Fe(2)-O(2)	154.1(3)	O(9)-Fe(4)-O(10)	156.0(2)
O(3)-Fe(2)-O(2)	94.2(2)	O(11)-Fe(4)-O(10)	94.7(2)
O(4)-Fe(2)-O(2)	74.3(2)	O(12)-Fe(4)-O(10)	74.7(2)
O(1)-Fe(2)-N(2)	89.1(3)	O(9)-Fe(4)-N(5)	86.4(2)
O(3)-Fe(2)-N(2)	85.5(2)	O(11)-Fe(4)-N(5)	92.1(2)
O(4)-Fe(2)-N(2)	77.6(2)	O(12)-Fe(4)-N(5)	106.5(2)
O(2)-Fe(2)-N(2)	109.9(2)	O(10)-Fe(4)-N(5)	76.5(2)
O(1)-Fe(2)-N(1)	86.0(2)	O(9)-Fe(4)-N(6)	90.8(2)
O(3)-Fe(2)-N(1)	91.2(2)	O(11)-Fe(4)-N(6)	86.3(2)
O(4)-Fe(2)-N(1)	107.5(2)	O(12)-Fe(4)-N(6)	76.1(2)
O(2)-Fe(2)-N(1)	76.3(2)	O(10)-Fe(4)-N(6)	107.0(2)
N(2)-Fe(2)-N(1)	173.1(2)	N(5)-Fe(4)-N(6)	176.3(2)

Table S5. Selected bond lengths (Å) and angles (°) for **5*R***.

Fe(1)-O(8)	1.997(3)	Fe(3)-O(5)	1.932(4)
Fe(1)-O(12)	2.001(3)	Fe(3)-O(7)	1.941(4)
Fe(1)-O(2)	2.002(3)	Fe(3)-O(6)	1.989(4)
Fe(1)-O(10)	2.014(3)	Fe(3)-O(8)	2.018(3)
Fe(1)-O(6)	2.029(3)	Fe(3)-N(4)	2.144(4)
Fe(1)-O(4)	2.057(3)	Fe(3)-N(3)	2.150(4)
Fe(2)-O(1)	1.933(4)	Fe(4)-O(9)	1.919(4)
Fe(2)-O(3)	1.939(4)	Fe(4)-O(11)	1.925(4)
Fe(2)-O(4)	2.011(3)	Fe(4)-O(10)	2.009(4)
Fe(2)-O(2)	2.011(3)	Fe(4)-O(12)	2.024(3)
Fe(2)-N(2)	2.135(4)	Fe(4)-N(6)	2.117(4)
Fe(2)-N(1)	2.138(4)	Fe(4)-N(5)	2.128(4)
O(8)-Fe(1)-O(12)	91.50(14)	O(5)-Fe(3)-O(7)	105.08(17)
O(8)-Fe(1)-O(2)	137.50(15)	O(5)-Fe(3)-O(6)	151.36(15)
O(12)-Fe(1)-O(2)	124.26(15)	O(7)-Fe(3)-O(6)	95.92(16)
O(8)-Fe(1)-O(10)	125.48(14)	O(5)-Fe(3)-O(8)	94.36(15)
O(12)-Fe(1)-O(10)	74.34(14)	O(7)-Fe(3)-O(8)	154.19(15)
O(2)-Fe(1)-O(10)	89.15(14)	O(6)-Fe(3)-O(8)	72.81(13)
O(8)-Fe(1)-O(6)	72.43(13)	O(5)-Fe(3)-N(4)	94.50(15)
O(12)-Fe(1)-O(6)	140.59(14)	O(7)-Fe(3)-N(4)	85.14(15)
O(2)-Fe(1)-O(6)	88.39(15)	O(6)-Fe(3)-N(4)	106.66(14)
O(10)-Fe(1)-O(6)	85.99(14)	O(8)-Fe(3)-N(4)	76.42(14)
O(8)-Fe(1)-O(4)	88.40(13)	O(5)-Fe(3)-N(3)	85.39(15)
O(12)-Fe(1)-O(4)	87.32(14)	O(7)-Fe(3)-N(3)	87.95(15)
O(2)-Fe(1)-O(4)	72.93(13)	O(6)-Fe(3)-N(3)	75.99(15)
O(10)-Fe(1)-O(4)	140.92(15)	O(8)-Fe(3)-N(3)	110.77(15)
O(6)-Fe(1)-O(4)	126.60(14)	N(4)-Fe(3)-N(3)	172.81(16)
O(1)-Fe(2)-O(3)	103.12(18)	O(9)-Fe(4)-O(11)	103.86(19)
O(1)-Fe(2)-O(4)	96.63(15)	O(9)-Fe(4)-O(10)	157.60(17)
O(3)-Fe(2)-O(4)	152.73(16)	O(11)-Fe(4)-O(10)	92.86(17)
O(1)-Fe(2)-O(2)	156.28(17)	O(9)-Fe(4)-O(12)	95.03(16)
O(3)-Fe(2)-O(2)	93.92(15)	O(11)-Fe(4)-O(12)	155.23(16)
O(4)-Fe(2)-O(2)	73.73(13)	O(10)-Fe(4)-O(12)	73.95(13)
O(1)-Fe(2)-N(2)	89.43(15)	O(9)-Fe(4)-N(6)	90.81(16)
O(3)-Fe(2)-N(2)	85.38(16)	O(11)-Fe(4)-N(6)	86.73(16)
O(4)-Fe(2)-N(2)	76.11(14)	O(10)-Fe(4)-N(6)	105.14(16)
O(2)-Fe(2)-N(2)	108.52(15)	O(12)-Fe(4)-N(6)	76.99(15)
O(1)-Fe(2)-N(1)	85.71(16)	O(9)-Fe(4)-N(5)	86.34(16)
O(3)-Fe(2)-N(1)	94.80(16)	O(11)-Fe(4)-N(5)	93.54(15)
O(4)-Fe(2)-N(1)	105.37(15)	O(10)-Fe(4)-N(5)	77.72(15)
O(2)-Fe(2)-N(1)	76.42(16)	O(12)-Fe(4)-N(5)	103.66(15)
N(2)-Fe(2)-N(1)	175.05(16)	N(6)-Fe(4)-N(5)	177.12(17)

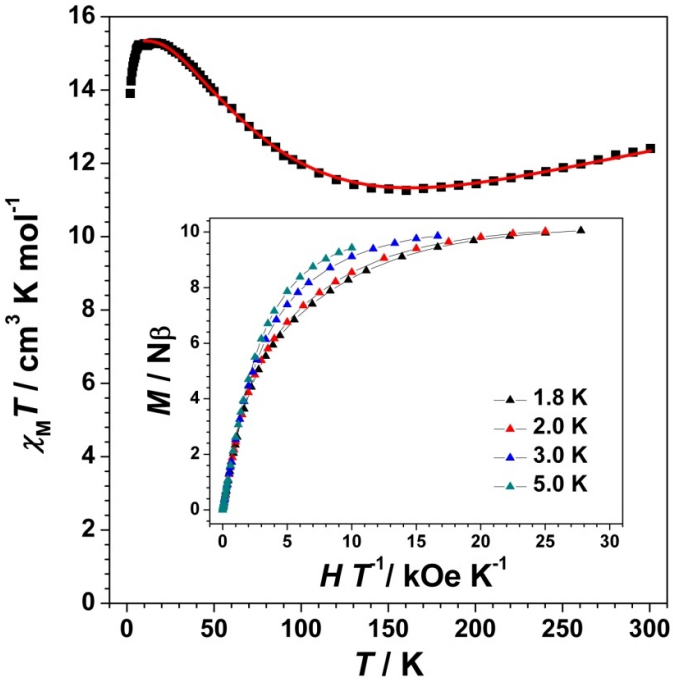

Figure S10. Temperature dependence of $\chi_M T$ at H = 1 kOe at 2–300 K (the red solid line represents the best simulation of magnetic susceptibilities calculated by MAGPACK at 10–300 K) and *M vs*. *H*/*T* plots at different temperature (1.8 K, 2 K, 3 K, and 5 K) for the polycrystalline sample of **2**.

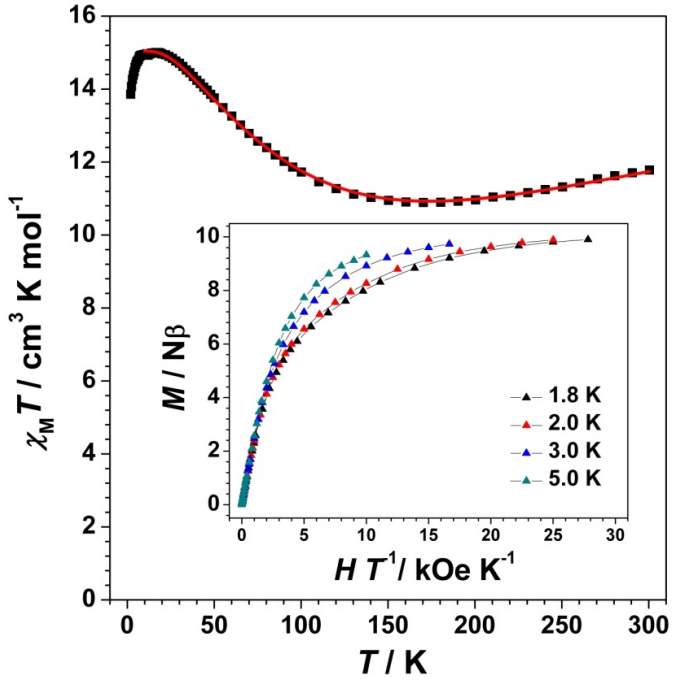

Figure S11. Temperature dependence of $\chi_M T$ at H = 1 kOe at 2–300 K (the red solid line represents the best simulation of magnetic susceptibilities calculated by MAGPACK at 10–300 K) and *M vs*. *H*/*T* plots at different temperature (1.8 K, 2 K, 3 K, and 5 K) for the polycrystalline sample of **3**.

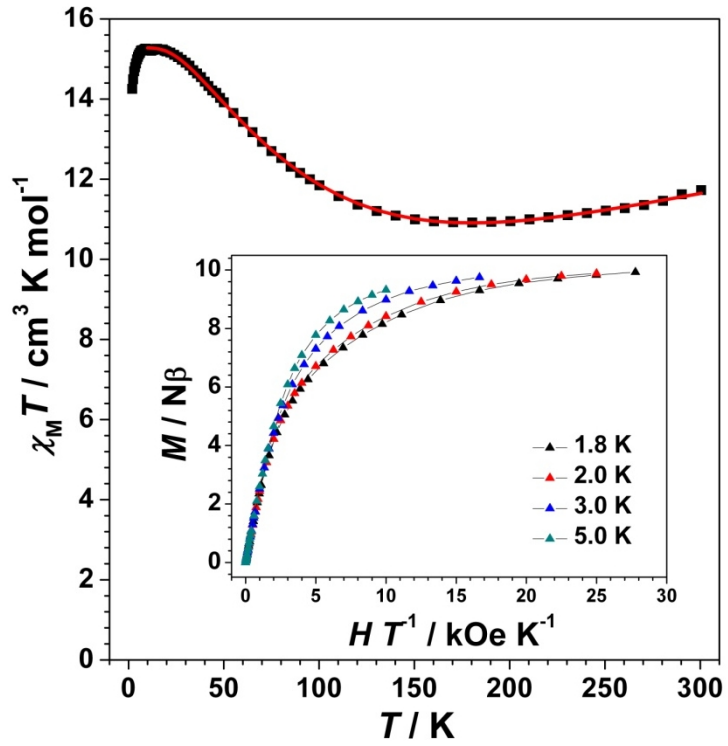

Figure S12. Temperature dependence of $\chi_M T$ at H = 1 kOe at 2–300 K (the red solid line represents the best simulation of magnetic susceptibilities calculated by MAGPACK at 10–300 K) and M *vs*. H/T plots at different temperature (1.8 K, 2 K, 3 K, and 5 K) for the polycrystalline sample of **5**.

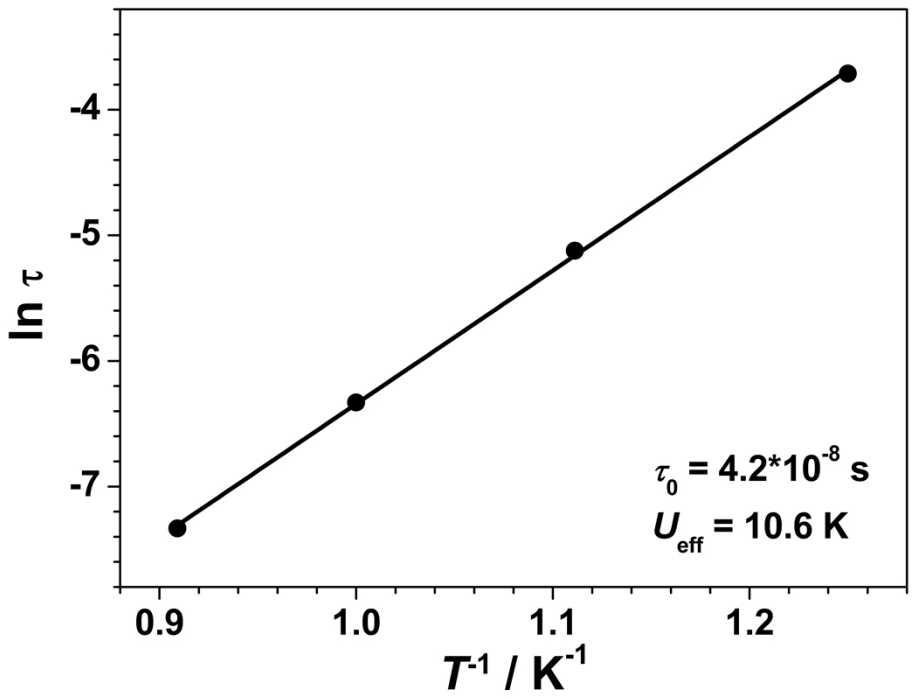

Figure S13. Arrhenius plots for compounds **4** obtianed from χ' *vs*. Frequency measurements in the absence of a dc field.

Table S6. The parameters of Cole-Cole fitting of **4** under zero applied dc field.

T (K)	X_0	X_t	τ	α	R
0.8	1.11006	25.83353	0.02246	0.29363	7.18×10^{-4}
0.9	0.64990	22.48040	0.00536	0.25137	5.04×10^{-4}
1.0	0.63406	20.09969	0.00175	0.20321	8.14×10^{-5}
1.1	0.34115	18.16938	0.00069	0.14653	2.37×10^{-5}

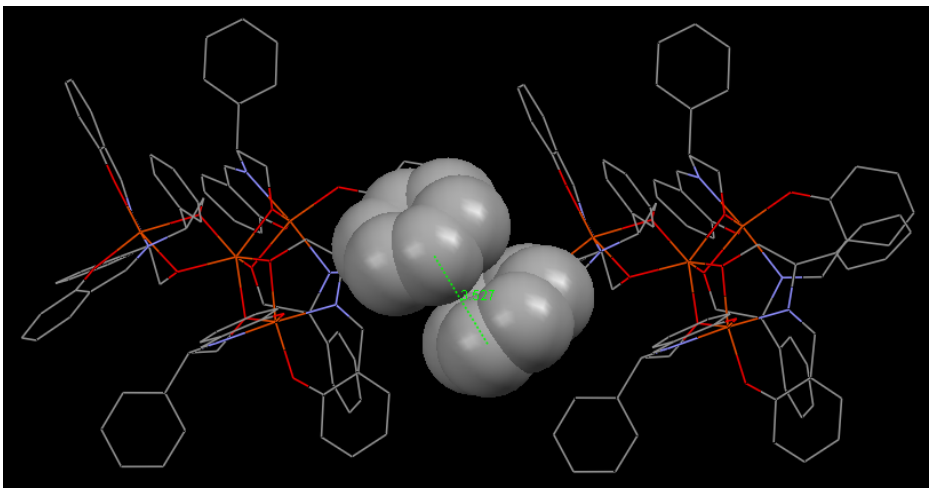

Figure S14. The π–π stacking of the benzene ring between the neighboring clusters in **1**.

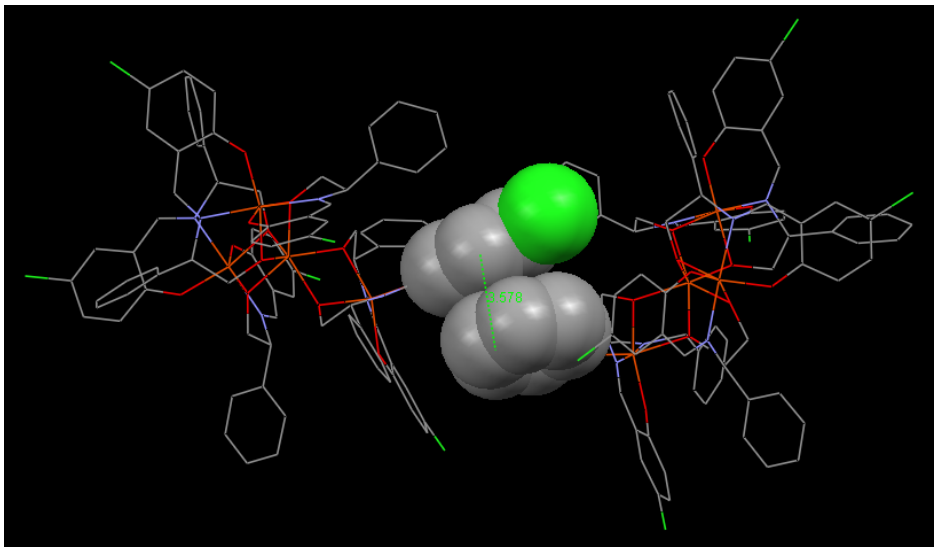

Figure S15. The π–π stacking of the benzene ring between the neighboring clusters in **2**.

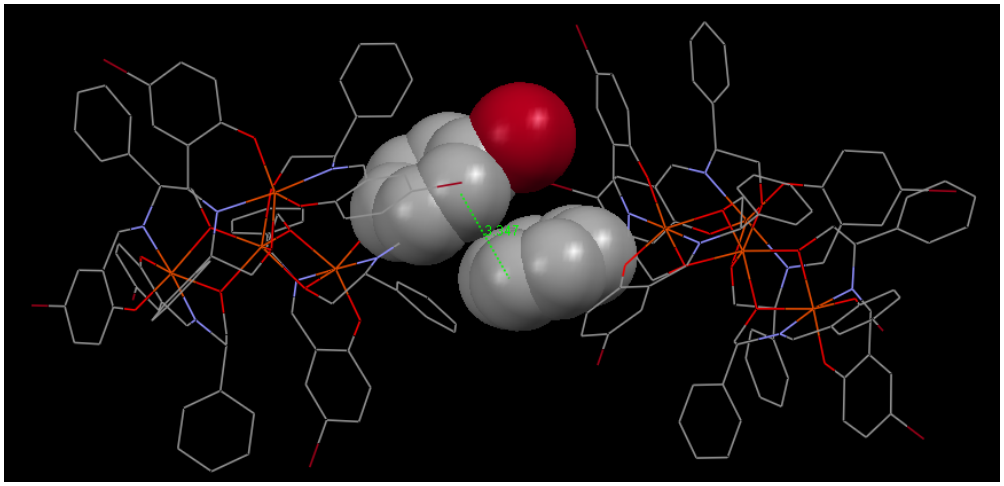

Figure S16. The π–π stacking of the benzene ring between the neighboring clusters in **3**.

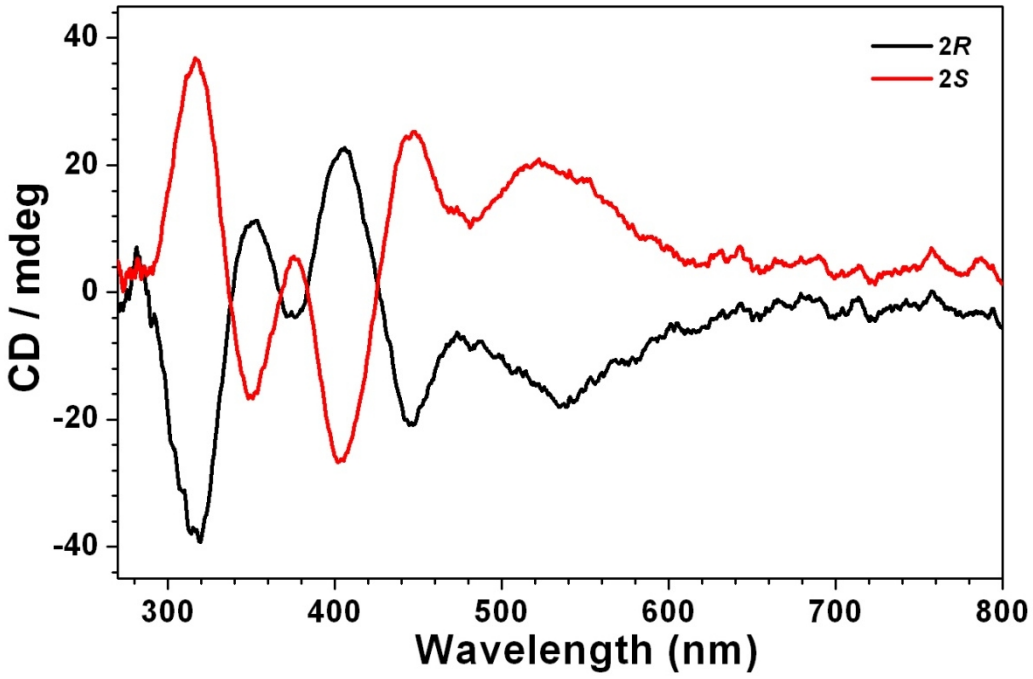

Figure S17. The solid-state CD spectra of **2*R*** (black) and **2*S*** (red) in KBr pellet at 298 K.

References:

1. Brewster, C. M.; Millam, L. H. *J. Am. Chem. Soc.* **1933**, *55*, 763–766.

2. Pavia, M. R.; Cohen, M. P.; Dilley, G. J.; Dubuc, G. R.; Durgin, T. L.; Forman, F. W.; Hediger, M. E.; Milot, G.; Powers, T. S.; Sucholeiki, I.; Zhou, S.-L.; Hangauer, D. G. *Bioorg. Med. Chem.* **1996**, *4*, 659–666.

3. Yu, X.-L.; Scheller, D.; Rademacher, O.; Wolff, T. *J. Org. Chem.* **2003**, *68*, 7386–7399.